

XRD and TEM characterization of the morphology of ZnO powders prepared by different methods

M. Markova-Velichkova¹, S. Veleva², V. Tumbalev¹, L. Stoyanov², D. Nihtianova^{1,3},
M. Mladenov², R. Raicheff², D. Kovacheva^{1*}

¹ Institute of General and Inorganic Chemistry, BAS - Acad. G. Bontchev str. Bd. 11

² Institute of Electrochemistry and Energy Systems, BAS - Acad. G. Bontchev str. Bd. 10

³ Institute of Mineralogy and Crystallography, BAS - Acad. G. Bontchev str. Bd. 107

Received February, 2013; Revised May, 2013

Three different synthesis techniques were applied in order to prepare ZnO powder samples with different crystallite size. The first method is thermal decomposition of $\text{Zn}(\text{NO}_3)_2 \cdot 6\text{H}_2\text{O}$. The second synthesis method is a sucrose-assisted solution combustion method. The third technique used is ultrasound assisted precipitation. A short-time thermal treatment is used to obtain ZnO materials with the required mean crystallite size. Materials were studied by means of powder XRD and TEM. The detailed morphology of the materials was first studied by XRD utilizing the special features of Fullprof program. This study revealed that different synthesis methods lead to products with different morphology. Materials obtained by the first method have an average crystallite size of 130–150 nm with irregular but isometric shape of the crystallites, while those obtained by the second method are almost spherical particles with size of about 30–40 nm. Regardless of the similar average crystallite size of the material obtained by the third method, its morphology is spindle-like, derived from different broadening of the XRD lines. The results from XRD analyses were confirmed by TEM observations. The influence of crystal morphology on the performance of ZnO as a main active material in zinc electrodes is discussed.

Key words: ZnO, synthesis, morphology, zinc electrodes.

INTRODUCTION

In recent years, many studies have been focused both on the synthesis and the morphological-structural characterization of new functional materials. Zinc oxide (ZnO) is a challenging inorganic material with various applications in many industrial branches, namely: in ceramic and rubber production; in electronics – for field emitters, gas sensors, ultraviolet lasers, solar cells, piezoelectric and optoelectronic devices; in chemical industry for photocatalysts; in energy production – for hydrogen-storage and alkaline batteries; and in environmental protection as biosensors, etc. [1–8]. Zinc oxide micro- and nanoparticles have attracted great interest due to their unique and remarkable chemical, electrical, mechanical, optical, and piezoelectric

properties. It was established that the properties and possible applications of the ZnO are strongly influenced by structure and morphology of the obtained products which depend on the method of synthesis and synthesis conditions [9–11]. Therefore, it is important to synthesize ZnO with different size and morphologies to explore its performance for certain applications. Experience in the use of ZnO in alkaline secondary batteries shows that many of the battery problems are related to the physical and electrochemical properties of ZnO. As an example, the initial morphology of the active ZnO anode material was found to influence strongly the electrochemical performance of the battery altogether. For example, the use of ZnO with prismatic shape improves the cycling life of the battery [12]. Many synthesis techniques are known for the ZnO preparation. Recently, several soft chemistry (*chimie douce*) methods have been developed, allowing modification of the morphology and the particle size, by affecting diameters and aspect ratios of ZnO particles. The aim of the present work is to obtain ZnO nanomaterial and to investigate the relation between

* To whom all correspondence should be sent:
E-mail: didka@svr.igic.bas.bg

its morphological characteristics and electrochemical properties. In the present work we also explore the ability of X-ray diffraction to obtain information about the crystallite morphology. This is possible by crystal structure refinement using the Rietveld method, where crystallite size and morphology are modeled with spherical harmonics.

EXPERIMENTAL

Three different techniques were applied in order to prepare ZnO powder samples with different crystallite size and morphology. The first method is thermal decomposition of $\text{Zn}(\text{NO}_3)_2 \cdot 6\text{H}_2\text{O}$. Aqueous solution of initial nitrate was placed in glass beaker and heated till evaporation. The obtained powders were heat-treated in air at 400 or 500 °C for 1 hour.

The second synthesis method is sucrose-assisted solution combustion method. For this purpose a $\text{Zn}(\text{NO}_3)_2 \cdot 6\text{H}_2\text{O}$ solution was mixed with sucrose-in-water solution in 1:1 ratio oxidizing to reduce the power ratio of the corresponding nitrates and organic fuel [13, 14]. The solutions were placed on a heating plate until evaporation of the water. After that, a foamy mass was formed, which produces an amorphous powder oxide material. The calculated average crystallite size of the as prepared sample is 5 nm. Consequently, materials were thermally treated in air at 350, 400 and 500 °C for 1h. Finally, the materials were grinded for homogeneity.

The third technique used is ultrasound-assisted precipitation. The sonication of the precipitate was performed by a 20 KHz, 750W ultrasonic processor SONIX, USA. The total sonication time was from 5 to 30 minutes. The obtained product was repeatedly washed with distilled water, filtered and finally dried at 80 °C.

Powder XRD patterns were recorded at room temperature on a Bruker D8 Advance diffractometer with Cu K_α radiation and LynxEye detector. TEM investigations were performed by transmission electron microscope JEOL 2100 at 200 kV accelerating voltage.

Electrochemical charge-discharge characteristics were collected using specialized laboratory cycling equipment allowing galvanostatic mode charge and discharge, as well as mixed mode constant current/constant voltage. Nickel electrode was commercial cathode produced in Bulgaria. Zinc electrode is prepared by introducing the zinc paste on the matrix (modified metallic or conductive ceramic composite). The pasted electrode is dried at 90 °C for 2 hours and then is pressed under 30 MPa for 2 min. Electrodes in the cell package are separated by a microporous polymer separator and immersed in alkaline (7M solution of KOH) electrolyte.

RESULTS AND DISCUSSION

This study revealed that different synthesis methods lead to products with different size and morphology. The diffraction patterns of ZnO materials obtained by the three methods are presented on Fig. 1. According to the X-ray diffraction patterns the products obtained through the first method are single phase ZnO. The average crystallite size of this material heated to 400 °C is about 100 nm. The increase of the temperature up to 500 °C leads to an increase in the crystallite size to about 150–200 nm.

The powders of ZnO prepared by the second method have crystallite size of about 6 nm. Additional heating to 400 and to 500 °C leads to an increase of crystallite size up to 10–12 and 25–30 nm, respectively. After one hour heat treatment at 600 °C, the sizes of crystallites were 45–50 nm. Thus this method allows easy preparation of ZnO material with predefined crystallite size.

The calculated mean crystallite size of the ZnO powders prepared by the third method is 24 nm. After thermal treatment at 600 °C for 1 h the mean crystallite size increases to about 50 nm. Powder diffraction pattern indicates the morphological peculiarities of this material. The diffraction peaks with indices (001) are significantly narrower than those with other indices, which mean larger size in this direction indicating rod-like or needle-like morphology of the crystallites.

The calculated crystallite sizes within the main directions and the calculated mean crystallite sizes are summarized in Table 1. The crystallite sizes within the main directions were estimated by single line fitting of the corresponding peaks with the

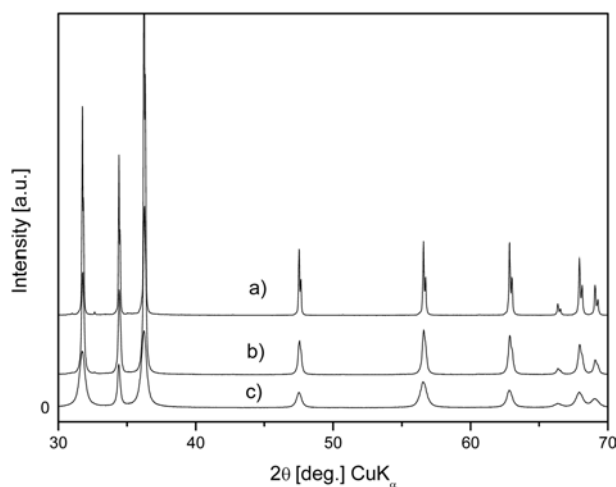


Fig. 1. XRD powder patterns of the materials obtained by the a) – decomposition; b) combustion; c) sonochemical methods

Table1. Calculated crystallite size within main directions of ZnO obtained by different methods

Line	100 (nm)	002 (nm)	101 (nm)	110 (nm)	Mean (nm)	$D_{(002)}/D_{(100)}$
ZnO – sonochemical as prepared	22	36	22	22	24	1.63
ZnO – sonochemical, heated	50	62	49	44	48	1.24
ZnO – combustion	52	49	46	50	47	0.94
ZnO – combustion (doped)	55	42	50	49	46	0.76
ZnO – decomposition	145	192	116	153	144	1.32

program Topas 4.2 [15] using the fundamental parameters peak shape description including appropriate corrections for instrumental broadening and diffractometer geometry.

Microstructural effects of materials may significantly hinder the successful crystal structure

determination via Rietveld refinement method. The standard peak profile functions as well as the Caglioti equation fit patterns of materials with isometric crystallites well, but when the morphology is somehow different from the spherical symmetry some peaks of the diffraction pattern could not be

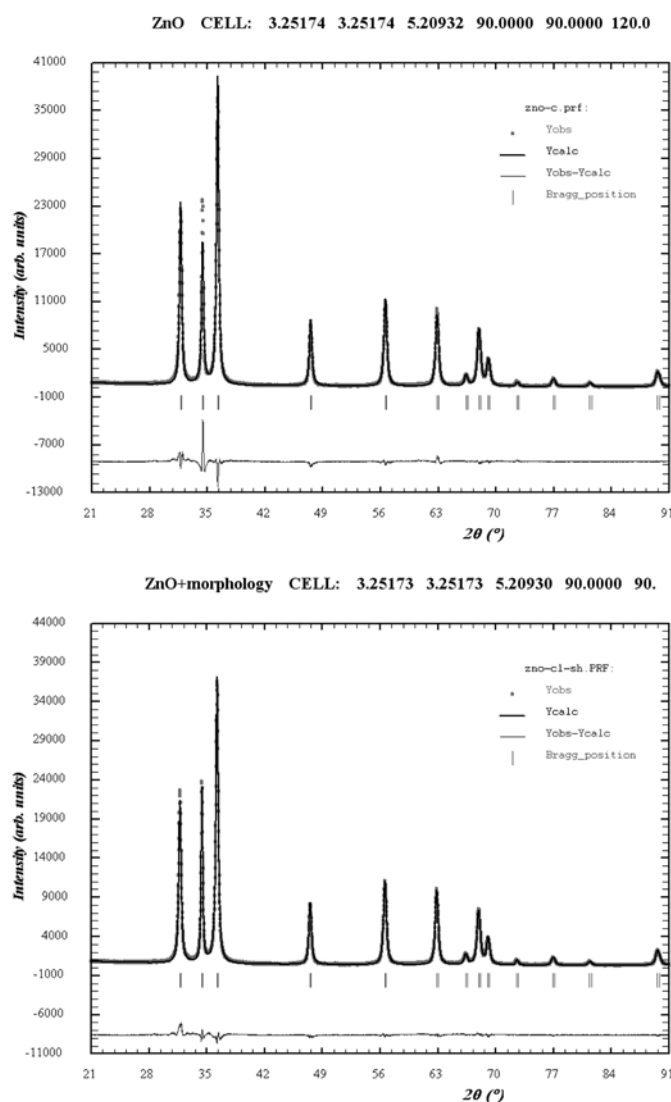


Fig. 2. Rietveld plot for ZnO obtained by the sonochemical method with the use of a) isotropic model for size broadening and b) using spherical harmonics

fit so good. As a result the refined structural parameters and their standard deviation may have values different from the expected ones for a well balanced structure. Such refinement may lead to unacceptable interatomic distances and highly distorted coordination polyhedra. Figure 2 illustrates the influence of microstructural effects by showing two Rietveld plots resulting from refinement of the crystal structure of ZnO using a) an isotropic model for size effects, and b) an appropriate crystallite morphology modelling.

The morphology of the materials synthesized by the three methods was first studied by XRD applying the special features of Fullprof [16] program. The microstructural effects in the program are introduced into the line broadening. For this purpose, instrumental and sample profiles are described by a convolution of Lorentzian and Gaussian functions, thus ensuring the simultaneous treatment of size and strain contribution to the line broadening. Spherical harmonics (SPH) are used for modeling the shape of the particles. Spherical harmonics are the angular parts of some solutions to Laplace's equation and they are widely used in different field of physics as a tool for gravitational, electric and magnetic fields description. In quantum chemistry they represent the atomic orbital electron configurations. Recently, spherical harmonics are used in the computer graphics in lightening effects and recognition of 3D shapes. The explicit formula for the SPH treatment of size broadening in Fullprof is the following [17]:

$$\beta_h = \frac{\lambda}{D_h \cos \theta} = \frac{\lambda}{\cos \theta} \sum_{lmp} a_{lmp} y_{lmp}(\Theta_h, \Phi_h)$$



Fig. 3. TEM photograph of ZnO prepared by the decomposition method

Where β_h is the size contribution to the integral breadth of reflection h , and $y_{lmp}(\Theta, \Phi)$ are the real spherical harmonics with normalization. For the proper use of this particular treatment of line broadening the instrumental resolution function should be preliminary determined by collecting the powder diffraction pattern of a standard sample with high crystallite size. After refinement of the coefficients the program calculates the apparent size (in angstroms) along each reciprocal lattice vectors.

It should be mentioned that the effect of the crystallite size on the broadening of diffraction lines is negligible for large crystallites (above 200 nm). As a result the attempt for modeling the size for the sample prepared from nitrate decomposition was not successful. Therefore, Transmission Electron Microscopy was used to confirm the findings of X-Ray diffraction. TEM photograph of the sample prepared by the decomposition method is presented on Fig. 3.

Figure 4a shows the XY, XZ and YZ projection of the “mean” crystallite as derived from XRD line broadening for ZnO prepared via the combustion method. TEM photograph of the ZnO prepared by this method is presented on Figure 4b. It can be seen that the particles are isometric, and that the shape derived from XRD analysis fits well with the shape observed in TEM.

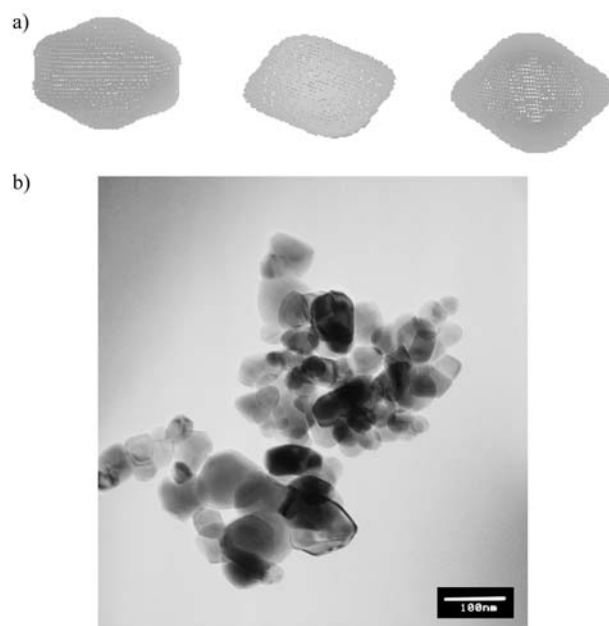


Fig. 4. a) XY, XZ and YZ projection of the “mean” crystallite, derived from the XRD line broadening for ZnO prepared via the combustion method; b) TEM photograph of ZnO prepared via combustion method

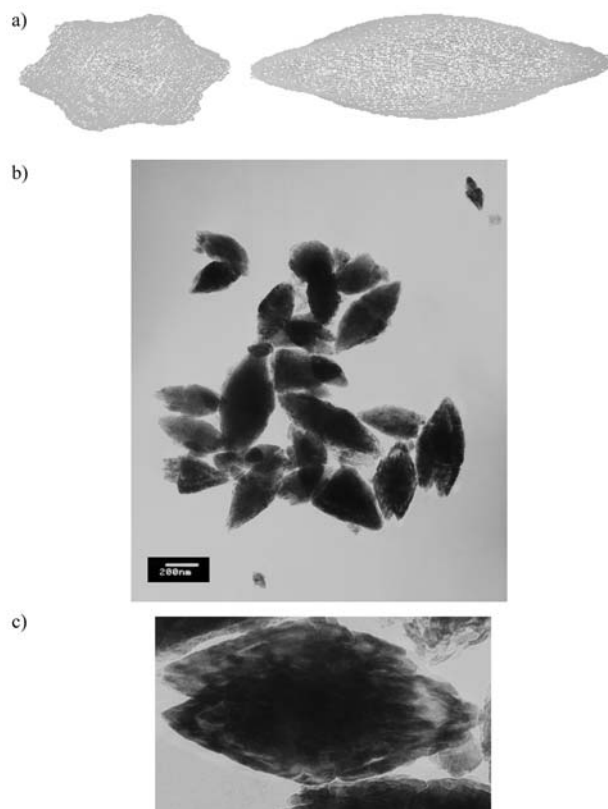


Fig. 5. a) The XY and XZ projection of the particles, derived from XRD line broadening for ZnO prepared via sonochemical method; b) TEM photograph of ZnO prepared by the sonochemical method; c) detail of the TEM photograph of ZnO prepared by the sonochemical method

A different morphology was observed for samples prepared via the sonochemical method. As it can be seen on Figure 5, both analytical methods give similar results representing spindle-like particles with different sizes within different crystallographic directions. The details in TEM photographs revealed also that spindle-like crystallites aggregate together with particles with same shape. Each big particle (with a size of about 200 nm) in fact consists of several smaller crystallites.

The electrochemical cycling behavior of pasted zinc electrodes with ZnO prepared by different methods is presented in Figure 6. The charge/discharge capacity of electrode with ZnO prepared via combustion method shows good stability during cycling as well as good capacity retention at different charge/discharge current rates. The initial capacity value for this material is about 200 mAh/g and decreases gradually to 180 mAh/g within 50 charge-discharge cycles at C/5 rate, where C is the theoretical capacity of ZnO (978 mAh/g). The increase of

the discharge rate to C/1.5 at charge rate C/2.5 lead to decrease of the capacity to about 75 mAh/g within the next 90 cycles. When the initial charge/discharge rate is restored, the capacity increases to its initial values. Cycling efficiency of this electrode is about 90–95%. Analogous behavior but higher values for the charge and discharge capacities (about 240 mAh/g) were observed for the capacity during cycling of electrodes with ZnO prepared via the sonochemical method. The dependence of charge and discharge capacity of the corresponding cell on cycle number demonstrates good electrochemical characteristics and cycling behaviour but relatively lower cycling efficiency (80–85%), compared to the zinc electrode with ZnO synthesized by combustion method. Nevertheless, the initial capacity of the ZnO prepared by decomposition method is relatively low (about 100 mAh/g) while the capacity fade during cycling is also very low.

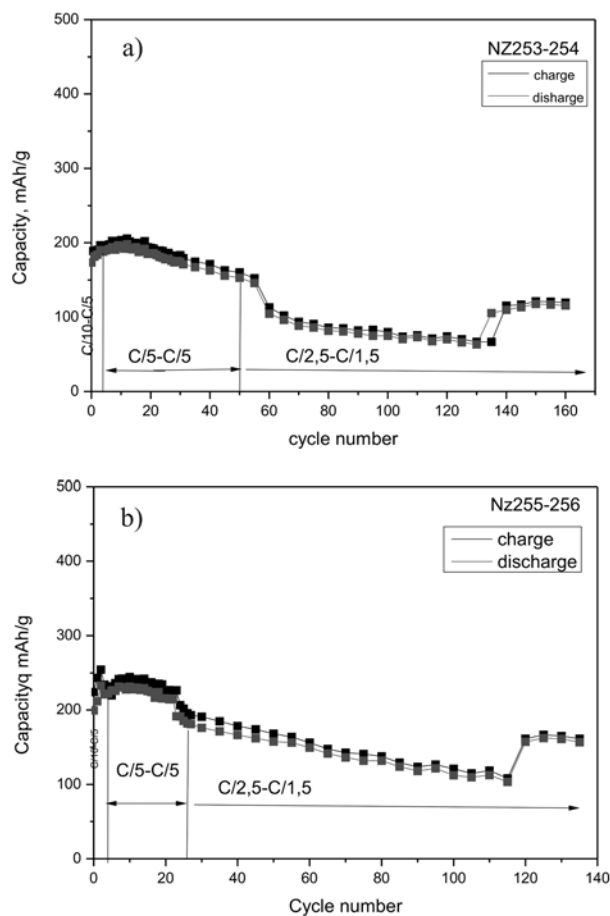


Fig. 6. a) Capacity during charge/discharge of electrode made with ZnO prepared via the combustion method; b) Capacity during charge/discharge of electrode made with ZnO prepared via sonochemical method

CONCLUSIONS

Compared to the conventional ZnO, nanosized ZnO anode material in Ni-Zn batteries shows better electrochemical characteristics – higher capacity and long cycling life. The reasons for such behavior could be attributed to higher specific surface area of the electrode prepared from nanoparticles thus ensuring better contact with the electrolyte. The morphology of the particles also influences the electrochemical behavior. ZnO with spindle-like particles showed higher capacity but lower electrochemical efficiency compared to ZnO with isometric particles.

REFERENCES

1. P. Yang, H. Yan, S. Mao, R. Russo, J. Johnson, R. Saykally, N. Morris, J. Pham, R. He and H.-J. Choi, *Adv. Funct. Mater.*, **12**, 323 (2002).
2. S. Chen, J. Zhang, X. Feng, X. Wang, L. Luo, Y. Shi, Q. Xue, C. Wang, J. Zhu, *Appl. Surf. Sci.*, **241**, 384 (2005).
3. J. Aranovich, D. Golmayo, A. Fahrenbruch, R. Bube, *J. Appl. Phys.*, **51**, 4260 (1980).
4. M. Wang, J. Wang, W. Chen, Y. Cui, L. Wang, *Mater. Chem. Phys.*, **97**, 219 (2006).
5. Y.W. Zhu, H.Z. Zhang, X.C. Sun, S.Q. Feng, J. Xu, Q. Zhao, B. Xiang, R.M. Wang, *Appl. Phys. Lett.*, **83**, 144 (2003).
6. K. Keis, C. Bauer, G. Boschloo, A. Hagfeldt, K. Westermark, H. Rensmo, H. Siegbahn, *J. Photochem. Photobiol. A Chem.* **148**, 57 (2002).
7. L. Luo, Y. Zhang, S.S. Mao, L. Lin, *Sens. Actuators A Phys.*, **127**, 201 (2006).
8. Y. Zhang, F. Zhu, J. Zhang, L. Xia, *Nanoscale Res. Lett.*, **3**, 201 (2008).
9. R. Wahab, Y.-S. Kim and H.-S. Shin, *Materials Transaction*, **50**, 2092 (2009).
10. S. Music, D. Dragcevic, S. Popovic, *J. of Alloys and Compounds*, **429**, 242 (2007).
11. Y. F. Yuan, J. P. Tu, H. M. Wu, Y. Z. Yang, D. Q. Shi, X. B. Zhao, *Electrochimica Acta*, **51**, 3632 (2006).
12. M. Ma, J. P. Tu, Y. F. Yuan, X. L. Wang, K. F. Li, F. Mao, Z. Y. Zeng, *Journal of Power Sources*, **179**, 395 (2008).
13. S. R. Jain, K. C. Adiga and V. R. Pai Verneker, *Combust. Flame*, **40**, 71 (1981).
14. M. M. A. Sekar and K. C. Patil, *J. Mater. Chem.*, **2**, 739 (1992).
15. TOPAS V4: General profile and structure analysis 14. software for powder diffraction data, User's Manual, Bruker AXS, Karlsruhe, Germany Bruker AXS (2008).
16. J. Rodríguez-Carvajal, FULLPROF: A Program for Rietveld Refinement and Pattern Matching Analysis, *Abstracts of the Satellite Meeting on Powder Diffraction of the XV th Congress of the International Union of Crystallography*, Toulouse, 127 (1990).
17. J. Rodríguez-Carvajal, Study of Micro-Structural Effects by Powder Diffraction Using the Program FullProf, *IV Congreso de la Sociedad Mexicana de Cristalografía*, Morelia, Michoacan, México, Libro de Resúmenes, 66 (2003).

РЕНТГЕНОГРАФСКО И ТЕМ ХАРАКТЕРИЗИРАНЕ НА МОРФОЛОГИЯТА НА ПРАХООБРАЗЕН ZnO, ПОЛУЧЕН ПО РАЗЛИЧНИ МЕТОДИ

М. Маркова-Величкова¹, С. Велева², В. Тумбалев¹, Л. Стоянов²,
Д. Нихтянова^{1,3}, М. Младенов², Р. Райчев², Д. Ковачева^{1*}

¹ *Институт по Обща и неорганична химия, БАН – ул. Акад. Г. Бончев, бл 11*

² *Институт по Електрохимия и енергийни системи, БАН – ул. Акад. Г. Бончев, бл 10*

³ *Институт по Минералогия и кристалография, БАН – ул. Акад. Г. Бончев, бл 107*

Постъпила февруари, 2013 г.; приета май, 2013 г.

(Резюме)

Поликристални образци от ZnO с различни размери на кристалитите бяха получени по три различни метода на синтез. Първият метод е чрез термично разлагане на $Zn(NO_3)_2 \cdot 6H_2O$. Вторият синтез е по метода на изгаряне от разтвор. Третата използвана техника е чрез ултразвуково третиране на утайка. Сравнително кратки времена на термична обработка са необходими за получаване на ZnO материали с желан среден размер на кристалитите. Материалите са изследвани с рентгенова дифракция и трансмисионна електронна микроскопия. Морфологията на материалите първоначално е изследвана с рентгенографски методи чрез прилагане на специалните възможности на програмата Fullprof. Изследването показва, че различните методи за синтез водят до получаване на продукти с различна морфология. Материалите, получени по първия метод имат среден размер на кристалитите 130–150 nm с неправилна но изометрична форма на кристалите, тези, получени по втория метод имат почти сферични частици с размер от около 30–40 nm. Въпреки същия среден размер на кристалитите на материала, получен по третия метод морфология на частиците е вретеновидна, съгласно резултатите от анализа на уширението на дифракционните линии. Резултатите от рентгенографските анализи бяха потвърдени от снимките получени от ТЕМ. Обсъдено е влиянието на морфологията на ZnO върху работата му като активен материал в цинкови електроди.